Structures 52 (2023) 17–29

Contents lists available at ScienceDirect

Structures

journal homepage: www.elsevier.com/locate/structures

Application of Machine Learning to predict the mechanical properties of high strength steel at elevated temperatures based on the chemical composition

Mohamed A. Shaheen [a,*], Rebecca Presswood [b], Sheida Afshan [b,*]

[a] School of Architecture, Building and Civil Engineering, Loughborough University, Loughborough, UK
[b] Faculty of Engineering and Physical Sciences, University of Southampton, Southampton, UK

ARTICLE INFO

Keywords:
Constitutive model
Elevated temperature
High strength steel
Machine Learning
Chemical Composition
Deep Learning

ABSTRACT

This paper presents the results obtained using Machine Learning (ML) algorithms to predict the mechanical properties, including ultimate tensile strength, yield strength, 0.2% proof strength and elastic modulus, of high strength steel plate material at elevated temperatures. High strength steels are increasingly used in several areas of construction offering efficient structural solutions with a high strength-to-weight ratio. Safe fire design of these structures relies heavily on accurate prediction of mechanical properties of the material with temperature. The data on elevated temperature mechanical properties collected from the literature experimental tests show a high degree of scatter, implying that they are influenced significantly by various factors, most notably the testing method, manufacturing process and chemical composition. However, the current methods for predicting the mechanical properties of high strength steels at elevated temperatures by using 'reduction factors' as adopted by the structural design codes do not consider these effects and may lead to inaccurate predictions. To overcome these deficiencies, a ML-based prediction method that uses temperature and chemical composition as input parameters is developed in this paper. Deep Neural Networks are trained and validated on the basis of elevated temperature material data collated from the literature test programmes. The analysis of the results show that the trained algorithm gives an excellent correlation coefficient with very small error value in predicting the strength and stiffness reduction factors of HSS.

1. Introduction

The use of high strength steel (HSS) in structural engineering applications has increased in recent years as it offers opportunities for both material and carbon savings. HSS enables structural designs with lighter supporting structures as well as layouts with more usable spaces. The thinner sections achieved with a higher strength steel require reduced welding effort and are easier to transport and construct. High strength steels are typically used in high rise construction, long-span structures and bridges where reduction of structural self-weight is paramount. High strength steels are defined as steels with yield strengths higher than 460 MPa within the European steel construction practice. The design of steel structures is currently covered in EN 1993-1-1 [1] for mild steel grades of S235 to S460 and in EN 1993-1-12 [2] for high strength steel grades of S500 to S700, where the digits represent the yield strength. In the second generation of Eurocodes the range of applicability of both of these design specifications will be increased to higher HSS grades, reflecting the greater knowledge and understanding gained from the recent research studies on high strength steel structures worldwide. EN 1993-1-1 will provide design rules for S235 to S700 grades, while EN 1993-1-12 will cover S700 up to S960 grades. The fire design of steel structures is covered in EN 1993-1-2 [3] for conventional strength steels. For HSS, EN 1993-1-12 currently states that the rules in EN 1993-1-2 are applicable to high strength steels up to S700.

The production of HSS is different from that of other steel types in two main aspects, the steel chemical composition and the heat treatment process that are adopted to achieve their higher strengths. There are four main processing routes for the production of high strength steel plates, namely: Thermo-Mechanical (TM) rolling, Thermo-Mechanical rolling with Accelerated Cooling (TM-ACC), Thermo-Mechanical rolling with Direct Quenching (TM-DQ) and Conventional route for QT plates [4]. The different chemical composition and heat treatment processes

* Corresponding authors.
E-mail addresses: m.shaheen@lboro.ac.uk (M.A. Shaheen), s.afshan@soton.ac.uk (S. Afshan).

https://doi.org/10.1016/j.istruc.2023.03.085
Received 30 August 2022; Received in revised form 30 January 2023; Accepted 15 March 2023
Available online 4 April 2023

employed in the production of HSS by these routes lead to material stress–strain behaviours that are different from those of conventional mild steels at both room and elevated temperatures. At room temperature, the ductility and the ratio of the ultimate-to-yield strength of HSS reduce with increasing strength. At elevated temperatures, high strength steels, like all steels, lose strength and stiffness with increasing temperatures, but the rate of degradation is influenced by the chemical composition and the heat treatment process.

The microstructure of mild steel can be either pearlite, bainite, or combination of both depending on the rate of cooling of austenite steel [5]. Bainite and pearlite transformations are stable phases, and do not transform to other phases without reheating to form austenite (at about 900 °C). On the other hand, the microstructure of HSS is martensite which forms when the austenite is rapidly cooled, or quenched, to a relatively low temperature in order to prevent carbon diffusion and hence the formation of pearlite or bainite. Martensite is not an equilibrium phase because the quenching process prevents diffusion of carbon out of the austenite structure. It tends to transform to stable ferrite and cementite phases when it is heated to a temperature (higher than 250 °C) that initiates diffusion of trapped carbon in the lattice [6]. The strength of HSS is controlled by the amount of developed cementite which is primarily a function of the chemical composition of the steel, the attained temperature and the duration of fire. Therefore, a combination of all of these factors, in particular the effect of chemical composition, need to be considered when predicting the elevated temperature mechanical properties of HSS materials.

2. Assessment of codified reduction factors

In structural design codes, elevated temperature material properties are typically expressed as a portion of the corresponding room temperature properties through reduction factors. The codified elevated temperature reduction factors are typically derived based on fitting the experimentally derived data points. However, there is typically a high degree of scatter in the measured elevated temperature mechanical properties as evidenced by the data from literature elevated temperature tests, plotted in Figs. 1 to 4. This scatter in the data is not systematically accounted for in the codified values. Moreover, the fitting methods do not specifically allow for the effect of chemical composition of the material on the elevated temperature mechanical properties, which is found to be an important factor especially for HSS and may therefore lead to their incorrect prediction.

To overcome the above mentioned limitations with the codified reduction factors, data-driven Machine Learning (ML) methods may be employed to predict the mechanical properties of HSS at elevated temperatures. M. Naser [7] adopted Machine Learning methods to predict the strength and stiffness of mild steel at elevated temperatures. A simple regression approach, where one parameter is included in the input layer, which was temperature, to predict one output, which was a reduction factor, was considered in their ML model. Desu et al. [8] adopted a multivariate regression approach to predict the mechanical properties of stainless steel 304L and 316L at elevated temperatures, which involved having more than one parameter in the input layer, which were various strain rates, to predict one output, which was a mechanical property. The trained ML models based on both the simple and the multivariant regression approaches adopted in these studies were found to successfully predict the mechanical properties at elevated temperatures, but a higher degree of accuracy was achieved for the multivariate regression.

3. Purpose of the study

The present study introduces a novel approach to derive strength and stiffness reduction factors for HSS at elevated temperatures using ML techniques. To the authors' knowledge, no prior studies are available in the open literature regarding the prediction of HSS mechanical properties at elevated temperatures by ML, particularly when the effect of material chemical composition is explicitly considered. A multivariate regression analysis approach is adopted which includes both the temperature and the chemical composition of the material in the input layer. The ML model is trained and validated on the basis of a database of elevated temperature material properties collected from published literature experimental programmes.

4. Data collection

A total of 366 data was collected from elevated temperature material testing programmes across 19 papers, covering high strength steel grades with nominal yield strengths ranging from 460 MPa to 960 MPa. Table 1 shows a summary of the key information related to the collected data experimental programmes. The elevated temperature tests included both steady state and transient state tests. Under steady state conditions, the specimen is heated to a specified temperature, then left for a period of time (holding time) until the temperature has stabilised and is then

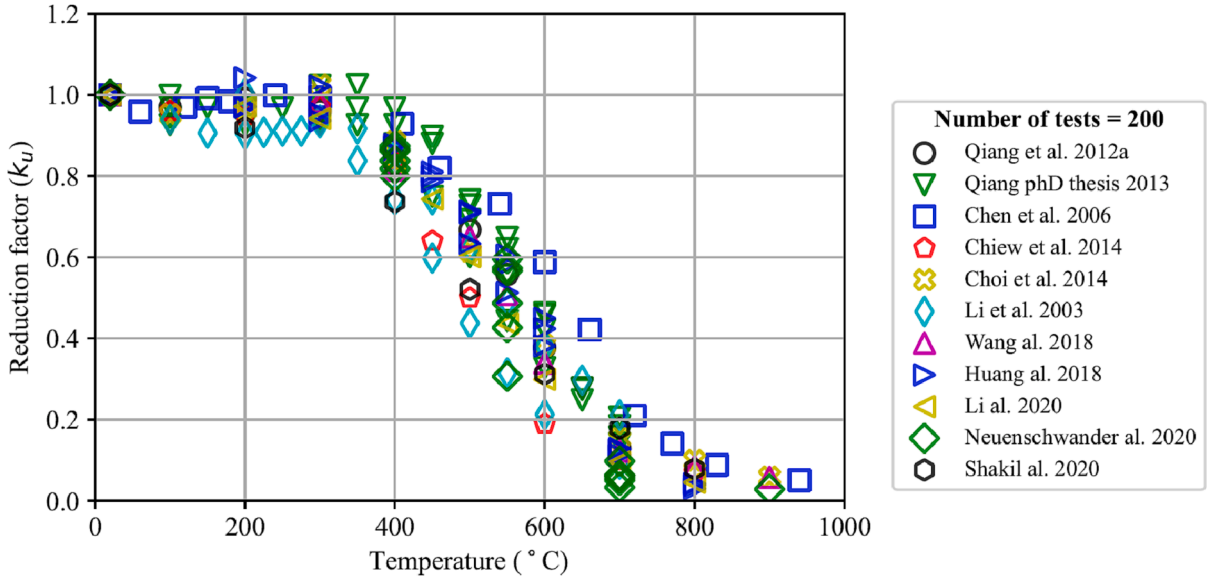

Fig. 1. Elevated temperature reduction factors for ultimate tensile strength.

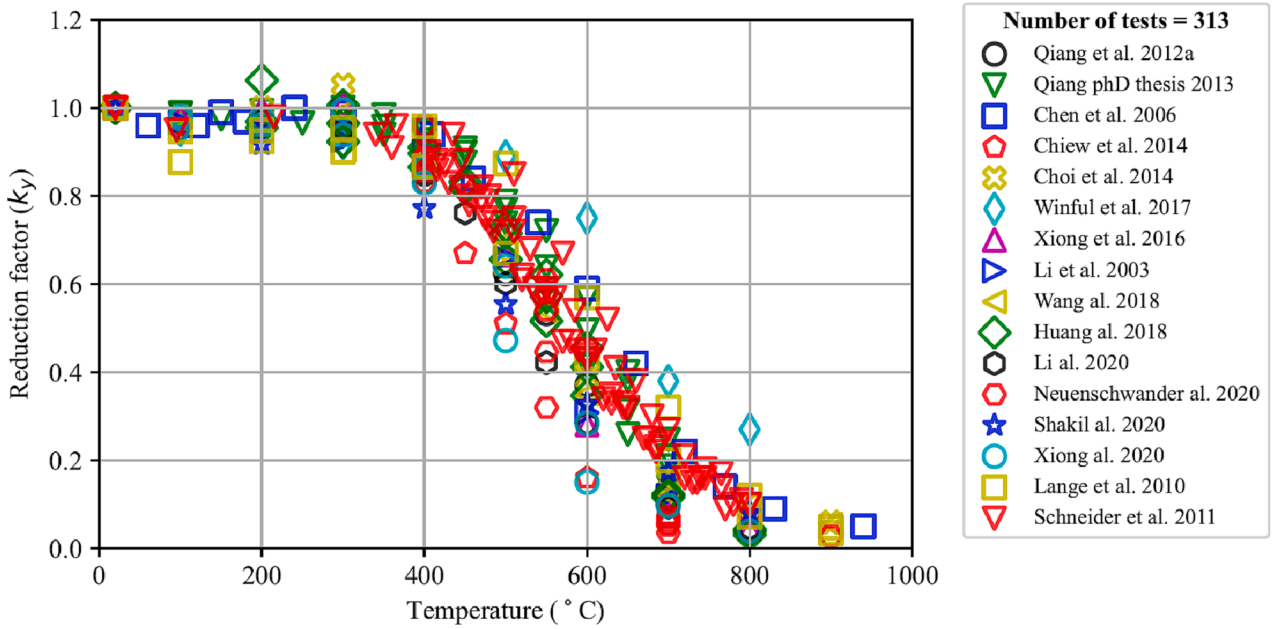

Fig. 2. Elevated temperature reduction factors for yield stress.

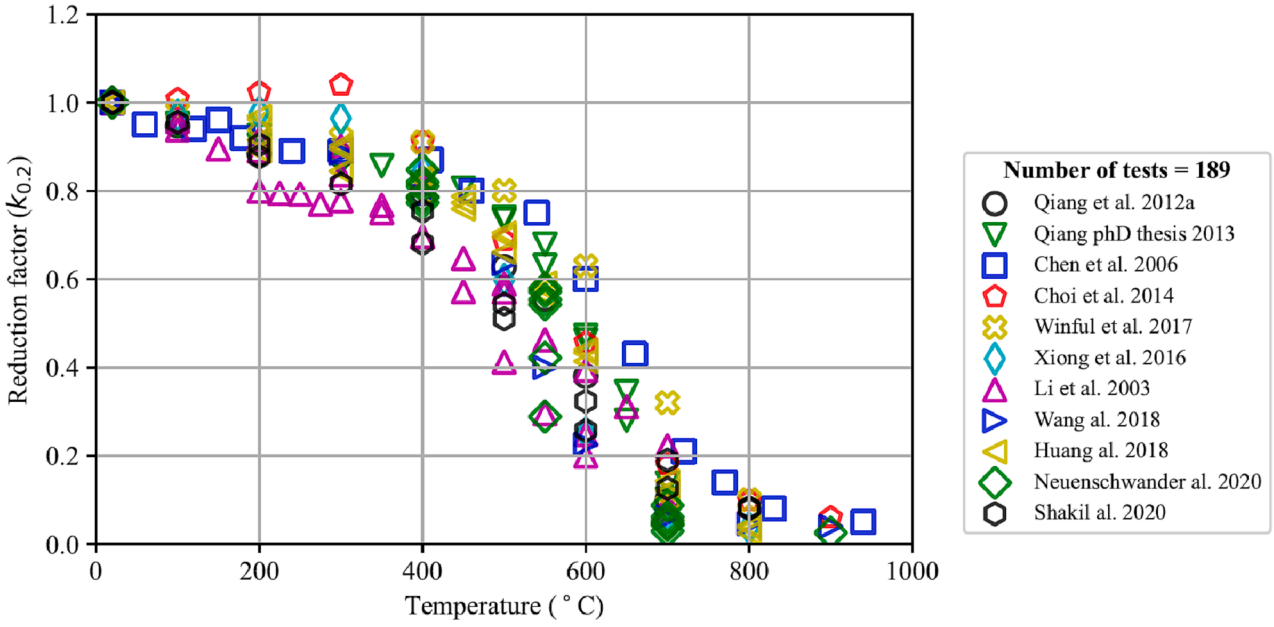

Fig. 3. Elevated temperature reduction factors for 0.2% proof stress.

loaded until failure whilst maintaining constant temperature as illustrated in Fig. 5**(a)**. Under transient state conditions, the specimen is loaded to a specified tensile load and then the temperature is increased as illustrated in Fig. 5**(b)**. Testing under transient state conditions more closely replicates the conditions that a structure is subject to during a fire, whereby the structure is already taking load when the temperature increases. However, steady state tests are easier to conduct in a laboratory and thus is the more common testing method. The heating rate and holding time for the tests were recorded where stated in the literature. Fig. 6 shows the variation in these parameters for each of the recorded tests; these discrepancies in testing methodology can be a source of scatter in the data.

Since high strength steels do not always demonstrate a clear yield point and a yield plateau in their stress–strain curves, the effective yield stress f_y was defined as the stress at 2% total strain. The 0.2% proof stress, $f_{0.2}$, is the stress at the intersection of the stress–strain curve with the proportional line offset by 0.2% strain, as illustrated by Fig. 7. **Equations (1)-(4)** present the definitions of the elevated temperature reduction factors for the ultimate tensile strength k_u, effective yield strength k_y, 0.2% proof strength $k_{0.2}$ and Young's modulus k_E that have been adopted throughout the analysis in this paper, where θ represents the temperature value.

$$k_u = \frac{f_{u,\theta}}{f_u} \tag{1}$$

$$k_y = \frac{f_{y,\theta}}{f_y} \tag{2}$$

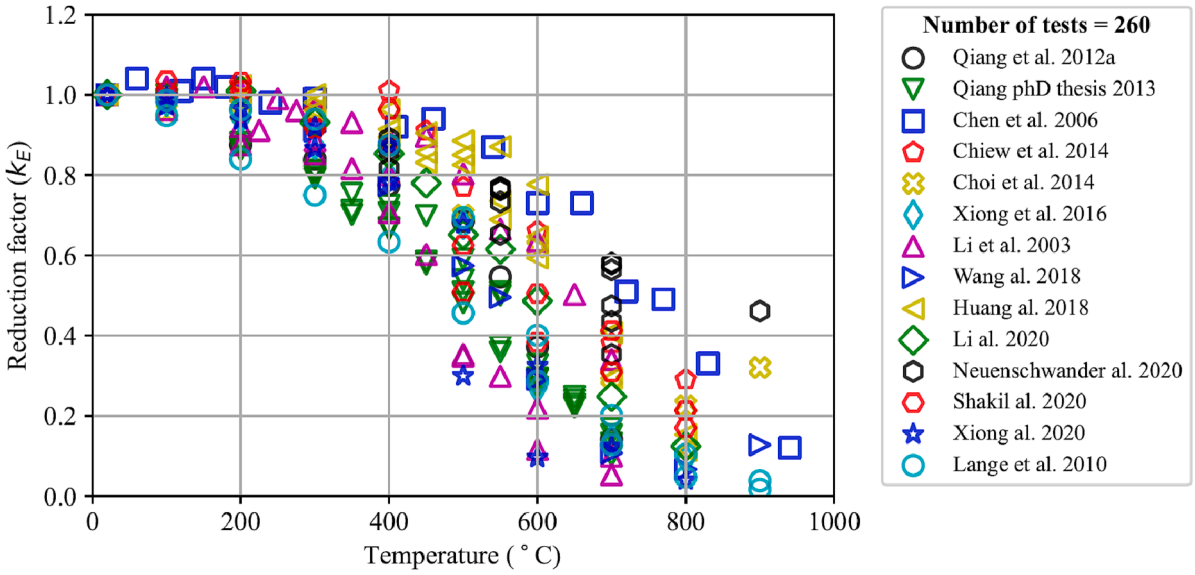

Fig. 4. Elevated temperature reduction factors for Young's Modulus.

Table 1
Summary of collected test data.

Ref.	Material type	Temperature range (℃)	Testing method	Heating rate (℃/min)	Holding time (min)	Nominal f_y (MPa)	Nominal f_u (MPa)	Number of tests
Qiang, Bijlaard & Kolstein, 2012a [9,11]	S690QL	20–700	Steady	50	10	690	770–940	9
			Transient	10	–			13
Qiang, Bijlaard & Kolstein, 2012b [10,11]	S460NL	20–700	Steady	50	10	460	550–720	12
			Transient	10	–			13
Qiang, 2013 [11]	S960QL	20–700	Steady	50	10	960	980–1150	10
			Transient	10	–			14
Chen, Young & Uy, 2006 [12]	BISPLATE80	20–940	–	–	–	620–690	720–930	16
Chiew, Zhao &Lee, 2014 [13]	S690 RQT	20–800	Steady	20	10	690	770–940	10
Choi, Chung & Kim, 2014 [14]	HSA800	20–900	Steady	10	10	650–770	800–950	10
Winful et al, 2017 [15]	S690 QL	20–800	Steady	Varies	15	690	770–940	9
Xiong & Liew, 2016 [16]	RQT701	20–700	Steady	10	60	690	770–940	9
			Transient	10	–			8
Li et al, 2003 [17]	20MnTiB	20–700	Steady	–	–	930	1130	10
Wang et al, 2018 [18]	Q690	20–900	Steady	20	20	690	770–940	9
Huang et al, 2018 [19]	Q550	20–800	Steady	20	15	550	640–820	10
	Q690					690	770–940	10
	Q890					890	940–11100	10
Jiang et al, 2019 [20]	Q690 CFD	20–900	Steady		20	690	770–940	10
Li & Song, 2020 [21]	Q690 TMCP	20–800	Steady	20	15	690	770–940	10
Neuenschwander et al, 2017 [22]	S690	20–900	Steady	15	30	690	770–940	12
	S960					960	980–1150	13
Shakil, Lu & Puttonen, 2020 [23]	S700MC	20–800	Transient	–	–	700	750–950	16
Wang et al, 2020 [24]	Q960E	20–900	Steady		20	960	980–1150	10
Xiong & Liew, 2020 [25]	S690 TMCP	20–800	Steady	10	30	690	770–940	9
			Transient	10	–			7
Schneider & Lange, 2011 [26]	S460	20–800	Transient	Varies	–	460	550–720	77
Lange & Wohlfeil, 2010 [27]	S460	20–900	Transient	10	–	460	550–720	20

Note: "-" means data not available.

$$k_{0.2} = \frac{f_{0.2,\theta}}{f_{0.2}} \tag{3}$$

$$k_E = \frac{E_\theta}{E} \tag{4}$$

The chemical compositions of the steel grades were also recorded for elements C, Si, Mo, Mn, Nb, Ni, Cu and Al. Figs. 8 to 10 show the chemical composition by weight for the steel grades 460 MPa, 690 MPa and 960 MPa steel, respectively. There is significant variation in the compositions of the steel, even within the same strength grade. This will also cause additional scatter in the data.

5. Development of the Artificial neural network (ANN)

Artificial neural networks (ANNs) consists of multiple layers and neurons that work together to process inputs and produce outputs. The number of neurons in each layer is determined by the complexity of the relationship between inputs and outputs. Supervised learning with a multilayer perception model with feed-forward back-propagation is used to develop an ANN in the present study. This model is composed of three layers: an input layer that contains the independent variables such as chemical composition and temperature, one or more hidden layers that establish relationship between the input and the output, and an output layer that contains the target variable such as strength reduction

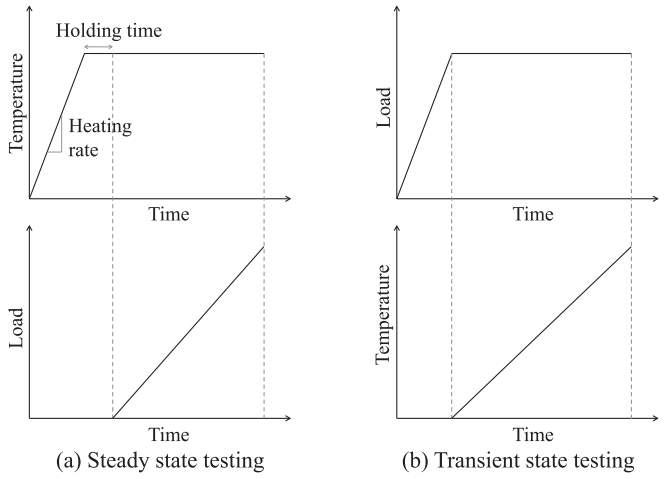

Fig. 5. Steady state and transient state test methods.

factors.

The training process for ANN begins by assigning random weight values to the connections between the input, hidden, and output layers. Input data is then inputted into the first layer's nodes and multiplied by the assigned weight values. These values are then passed through a transfer function, such as a sigmoid function, and the output is used to make predictions. These predictions are then compared to known values and the error between them is calculated. This error is then used to adjust the weight values through a process called backpropagation and the process is repeated until the predicted outputs match the known values within an acceptable range.

Fig. 11 illustrates the neural network architecture comprising the input layer, hidden layers, and output layer. Each layer can have one or more connected neurons passing signals to each other based on the received input and form a complex network that learns with some feedback mechanism. The connection between any two neurons would have an associated weight which defines the influence of the input to the output for the next neuron and eventually for the overall final output. To derive an effective neural network architecture, a number of parameters need to be introduced including, input variables, the number of hidden layers and the associated number of neurons, the activation function, the number of epochs, and the output variables. These parameters are generally identified through trial-and-error loops until the model is well generalized. However, there are some guidance available in the literature to find an effective architecture with minimal number of loops [28].

The input layer receives input parameters governing a phenomenon. It should be pointed out that both multivariate and simple regression models were considered in this study to give an insight into the importance of using chemical composition and holding time in addition to temperature in predicting the elevated temperatures reduction factors. The chemical composition input variables for the multivariate model (see Fig. 11) included the main elements C, Si, Mo, Ni. The other chemical compositions shown in Figs. 8-10 were not considered as they were absent in several publications. It should be noted that the phase transformation during the fire is affected by the time exposure duration and thus the holding time under which the tests were performed was also considered as an input variable for the steady state tests dataset. The input layer for the simple model only included the temperature. The input layer is then connected to successive hidden layers through nonlinear activation functions such as Sigmoid and leads onto the output layer, which in this case is the predicted values of the elevated temperature reduction factors, k_u, k_y, $k_{0.2}$ or k_E, of high strength steel plate material for both models. The input variables were initially normalised within the range of 0.0–1.0 using **Equation (5)** to improve the learning speed, accuracy, and the convergence rate.

$$X_n = \frac{X - X_{min}}{X_{max} - X_{min}} \tag{5}$$

where, X_{min} and X_{max} are the minimum and maximum values of input X, and X_n is the normalised data of the corresponding X. The normalised data is then returned to the original value using **Equation (6)** after the best trained network is obtained.

$$X = X_n(X_{max} - X_{min}) + X_{min} \tag{6}$$

The experimental data is randomly divided into three parts for training, validation, and testing process – 70% of the collected data was

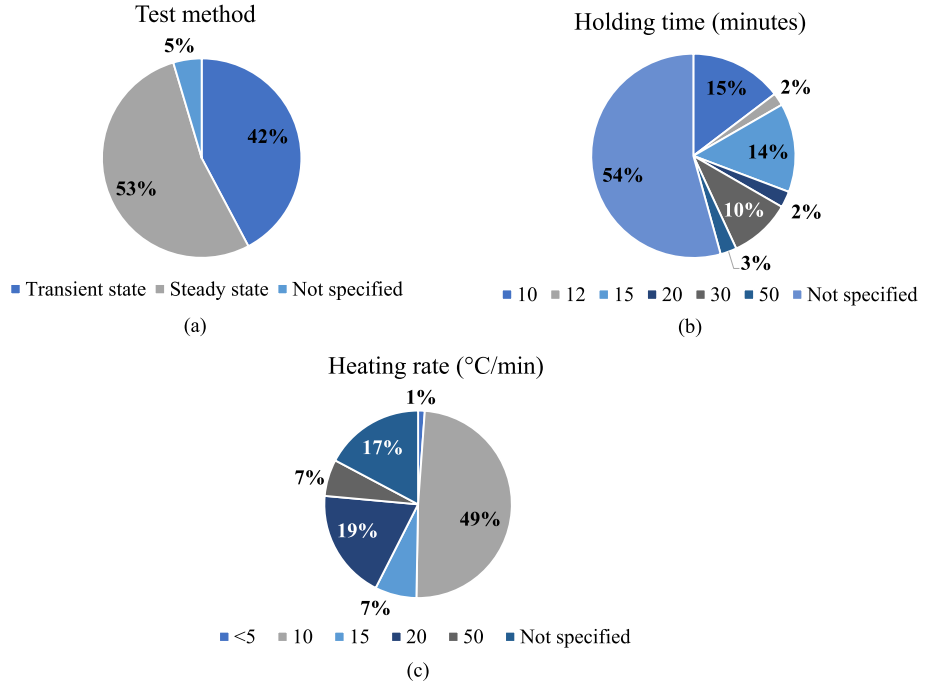

Fig. 6. **(a)** Proportion of steady state and transient states, **(b)** Variation in holding time and **(c)** Variation in heating rate from collected test data.

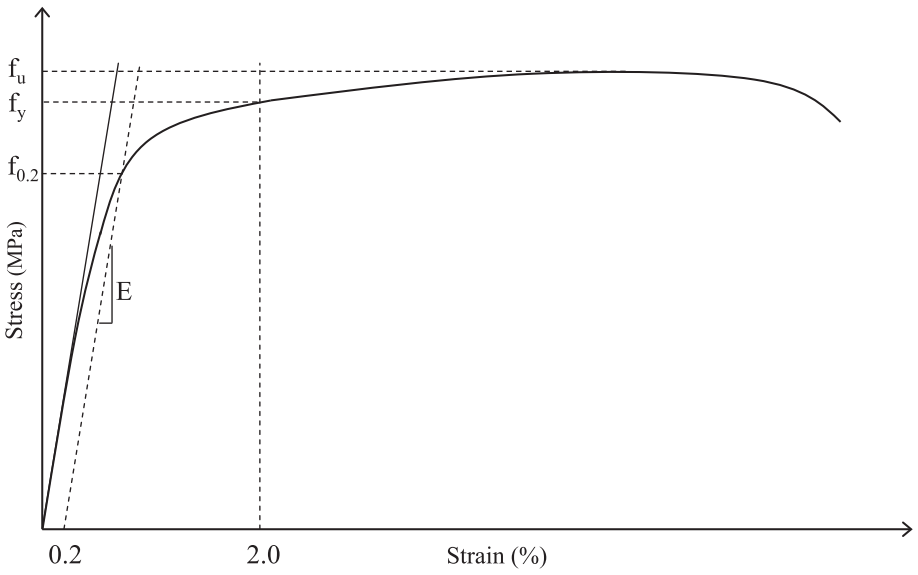

Fig. 7. Typical stress–strain curve for high strength steels.

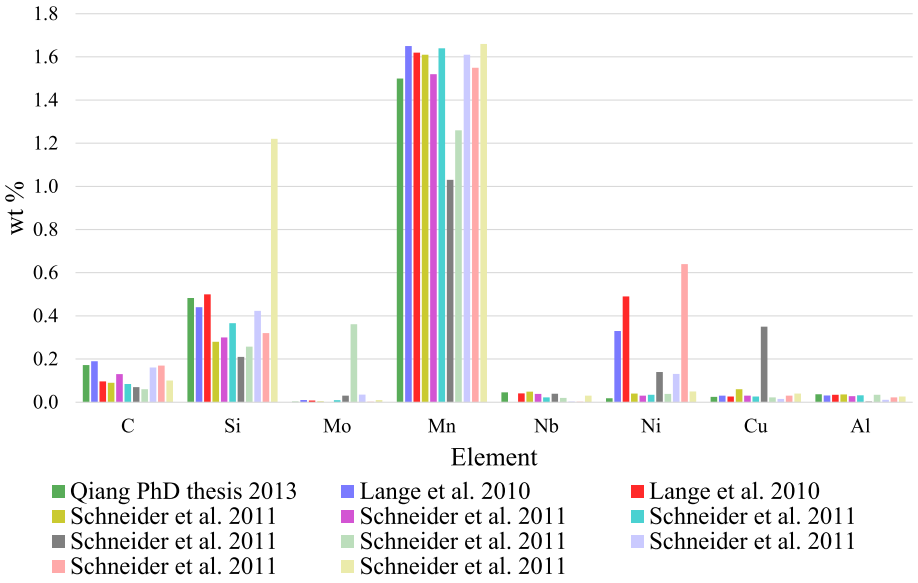

Fig. 8. Chemical composition wt% for steel grades with nominal yield strength 460 MPa.

used to train the model, of which 15% was used for validation, and the remaining 30% was used to test the performance of the developed model. A good model will have the ability to digest new data and make accurate predictions; this can be achieved by generalising the model and avoiding overfitting or underfitting. Although adopting many neurons in the hidden layers improves the accuracy of the model, this requires more computational time and may also lead to undesirable overfitting.

6. Performance and validation of derived material models

Following the training of the model, the performance of the trained network was assessed by comparing the predicted and experimental values of the reduction factors for the whole database. To assess the accuracy of the model, two parameters, the coefficient of determination (R^2) and mean absolute errors (MAE), are considered. R^2 is a statistical measurement that examines the goodness of fit of a linear relationship between the predicted and experimental values which is calculated using **Equation (7)**.

$$R^2 = 1 - \frac{\sum_{i=1}^{n}\left(y_p^i - y_{exp}^i\right)^2}{\sum_{i=1}^{n}\left(y_{exp}^i - y_{mean}^i\right)^2} \tag{7}$$

where, y_{exp} is the experimental value, y_p is the predicted value, y_{mean} is the mean value of the experimental data, and n is the total number of data points being considered. The coefficient of determination alone is not sufficient to validate the trained model. The predictions of the model may be biased towards higher or lower values. Thus, MAE between the predicted and the experimental values is also considered which can be calculated by **Equation (8)**, where the symbols are as previously defined.

$$MAE = \frac{\sum_{i=1}^{n}\left|y_p^i - y_{exp}^i\right|}{n} \tag{8}$$

Table 2 summarises the coefficient of determination (R^2) and the mean absolute errors (MAE) for the training and the testing data sets for

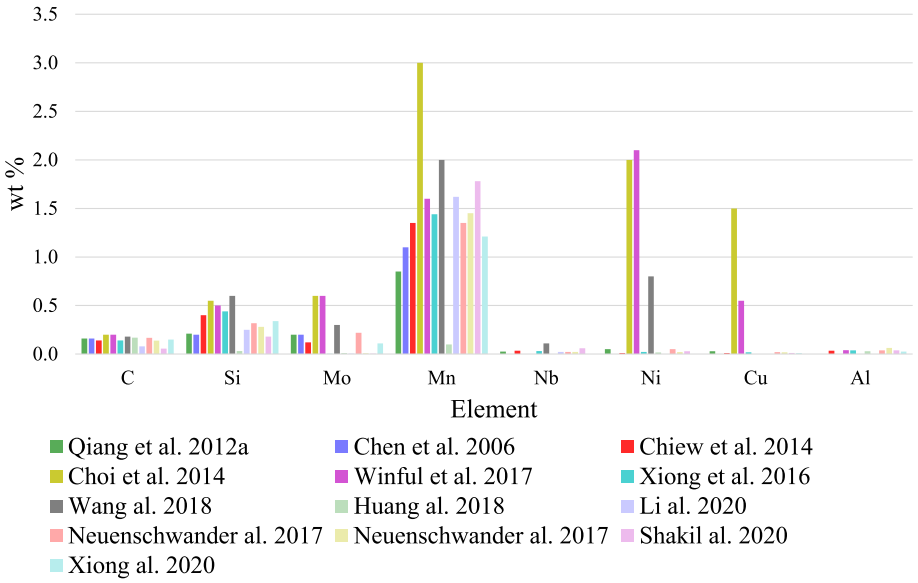

Fig. 9. Chemical composition wt% for steel grades with nominal yield strength 690 MPa.

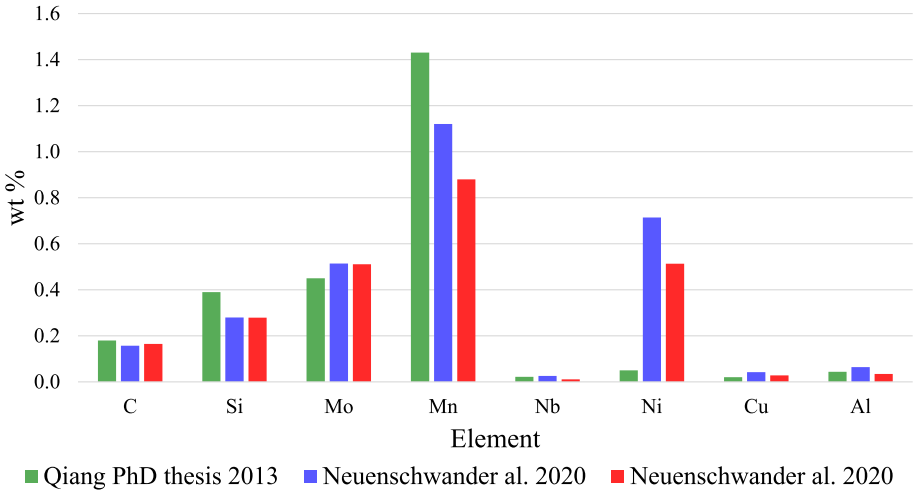

Fig. 10. Chemical composition wt% for steel grades with nominal yield strength 960 MPa.

the multivariate and simple models. The multivariate training model is shown to have excellent predictive accuracy as the R^2 values for all the reduction factors are above 0.92 and the MAE values are negligible. Despite the R^2 values for the simple model being comparable with those of the multivariate model, the MAE values of the simple model are significantly higher, particularly for the testing data set. This implies that the R^2 alone is not sufficient to evaluate the model performance. Section 5 provides a detailed comparison between the multivariate and simple regression models considered in this study. Fig. 12 presents the multivariate predicted versus the experimental values for all the considered reduction factors, where it is shown that for both the training and testing datasets, the predicted data points lie within a ±10% bound. It is also clear from Table 2 and Fig. 12 that the model prediction for the training and the testing data set are comparable and hence indicating that the model is well generalised. Thus, it can be concluded that the multivariate model can predict the strength reduction factors of high strength material with good accuracy.

7. Comparison of simple and multivariate models

To evaluate the effect of considering the chemical composition of the material on the predicted elevated temperature reduction factors, a comparison between the predicted values using simple regression (i.e. including temperature only in the ANN model) and multivariate regression (i.e. including temperature and chemical composition in the ANN model) is shown in Fig. 13 for both the training and the testing datasets. Both the simple and the multivariate regression methods depict the trend of the experimental values. However, the former predicts only a single reduction factor at each temperature that fits precisely between the collected observations, while the latter provides various reduction factors at each temperature depending on the chemical composition of the material.

Tables 3 and 4 compares the experimental values of the ultimate tensile strength reduction factors with the predicted values from the above-described simple and multivariant regression methods together with their corresponding errors, where $k_{u,\exp}$ is the experimental ultimate tensile strength reduction factor, $k_{u,m}$ and $k_{u,s}$ are the corresponding predicted reduction factors by the multivariate and simple regression methods, respectively and $\rho_{u,m}$ and $\rho_{u,s}$ are the percentage errors for the multivariate and simple regression methods, respectively. Reduction factors for temperatures below 350 °C are not included in the table as the scatter in the test data is not significant and the predictions

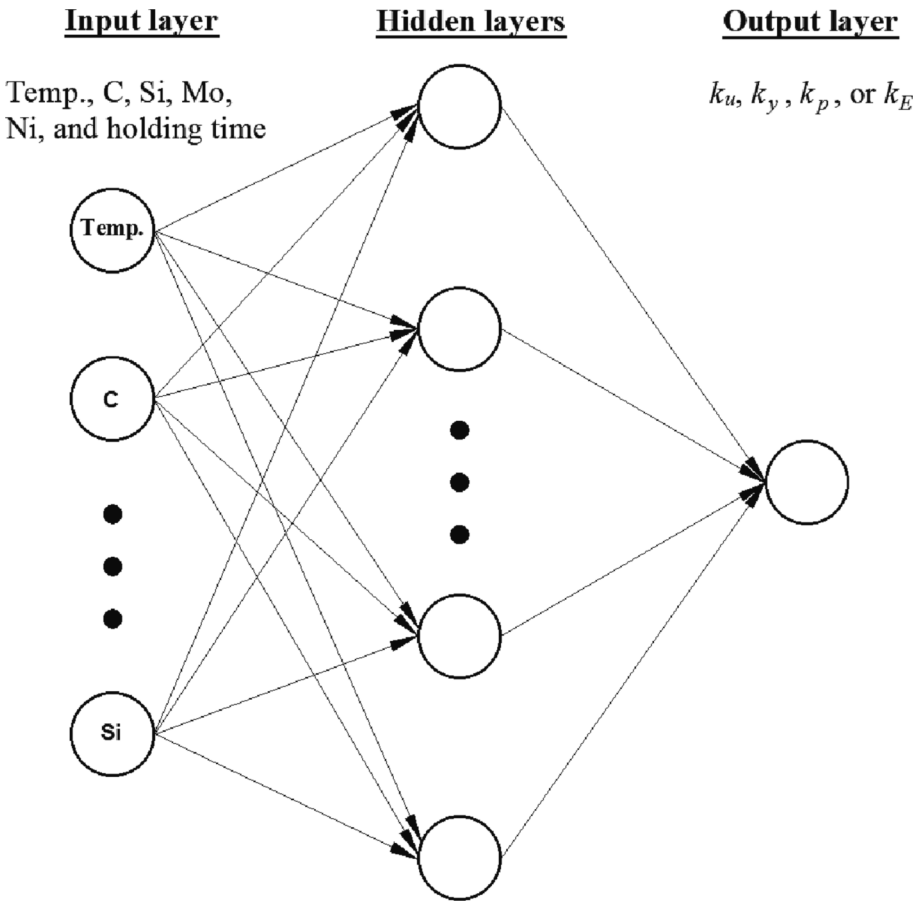

Fig. 11. The adopted ANN Model with 4 neurons in the hidden layer for the multivariate model.

Table 2
Statistical parameters for the training data.

Property reduction factor	Multivariate model				Simple model			
	Training data		Testing data		Training data		Testing data	
	R^2	*MAE*	R^2	*MAE*	R^2	*MAE*	R^2	*MAE*
Tensile strength (k_u)	0.98	0.030	0.99	0.023	0.97	0.038	0.95	0.047
Yield stress (k_y)	0.98	0.030	0.98	0.029	0.98	0.031	0.94	0.056
Proof stress ($k_{0.2}$)	0.98	0.035	0.98	0.028	0.96	0.054	0.97	0.039
Young's modulus (k_E)	0.92	0.039	0.93	0.038	0.86	0.084	0.81	0.084

by the two regression methods are comparable. From Tables 3 and 4, the percentage error for both regression methods is relatively small at the low temperatures e.g. at 400 °C, the percentage error is less than 12% and 18% for multivariate and simple regression methods, respectively. However, at high temperatures, larger than 400 °C, high strength steels exhibit different elevated temperature performance depending on the chemical composition of the material, which in turn results in a significant scatter in the collected data. Having merely a single prediction at each temperature by adopting the simple regression method results in a significantly large error. For example, the simple regression method predicts ultimate tensile strength reduction factors 67% and 325% higher than the actual value at 550 °C and 700 °C, respectively. Adopting the multivariate method reduces the gap between the predicted and the actual values by predicting several reduction factors at the same temperature; reducing the absolute errors at 500 °C and 700 °C to 20% and 80%, respectively. The multivariate predicted values at 800 °C and 900 °C are comparable with those predicted by the simple regression method due to the limited data availability. Thus, the accuracy can be increased by feeding further data to the model. The above presented discussion is also applicable to the other reduction factors of k_y, $k_{0.2}$ and k_E.

8. Effect of chemical composition on the strength reduction factor

Fig. 14 depicts the absolute average error at various temperatures for ultimate and yield strength reduction factor predictions when different chemical composition was separately used in the ML algorithm, along with those corresponding to predictions without considering the chemical composition. The reduction factors can be accurately predicted at low temperature (500 °C) without considering the chemical composition as various models show approximately similar errors. However, the reduction factors show significant dependency on the chemical composition at high temperature, particularly between the temperature range of 600 °C and 900 °C. Furthermore, various chemical compositions predict the ultimate strength reduction factor with different accuracy. For example, the best correlation with the tested value was obtained when Ni was used in the ML algorithm while Si shows a poor

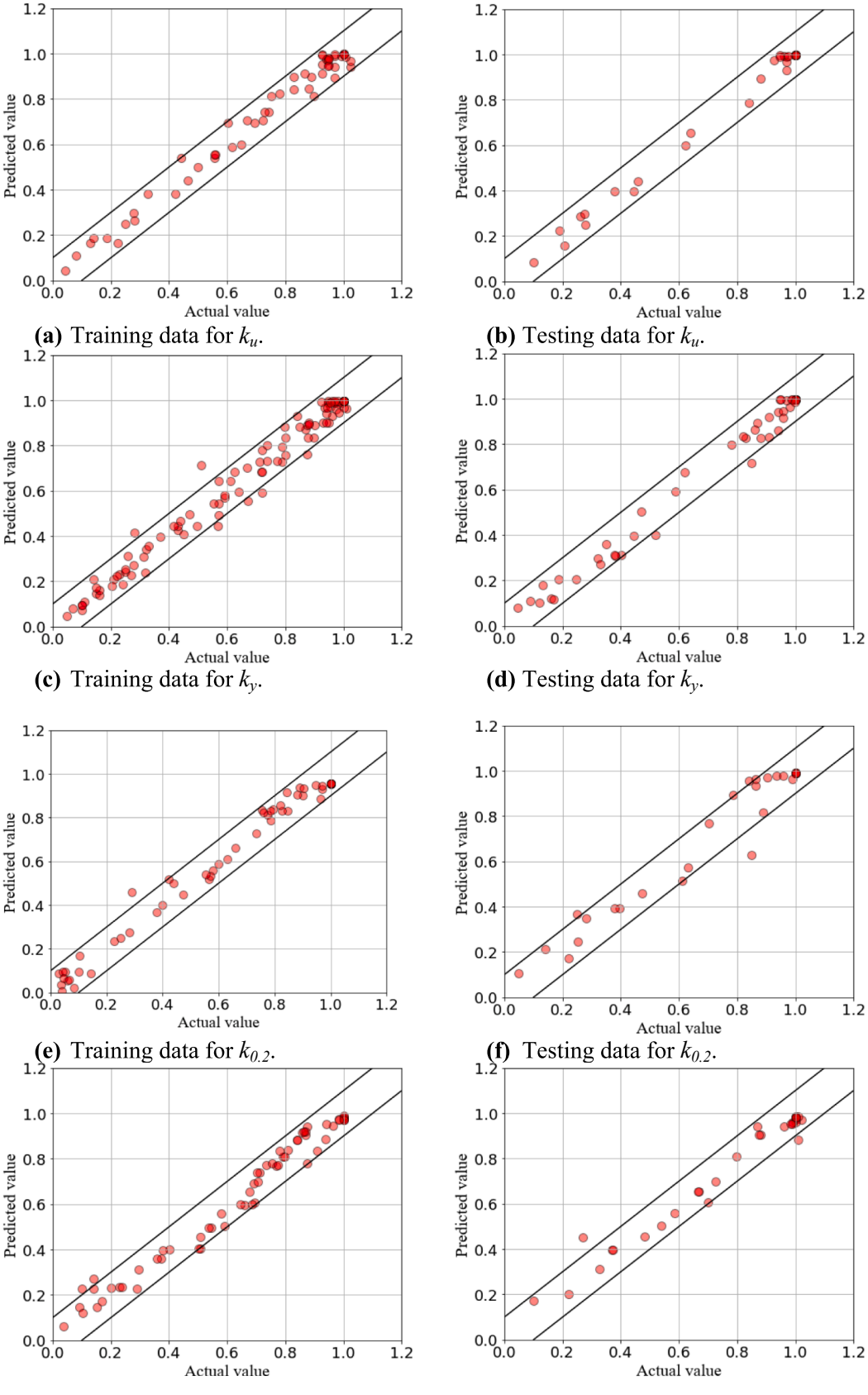

(a) Training data for k_u.

(b) Testing data for k_u.

(c) Training data for k_y.

(d) Testing data for k_y.

(e) Training data for $k_{0.2}$.

(f) Testing data for $k_{0.2}$.

(g) Training data for k_E.

(h) Testing data for k_E.

Fig. 12. Accuracy of the developed model for the material reduction factors.

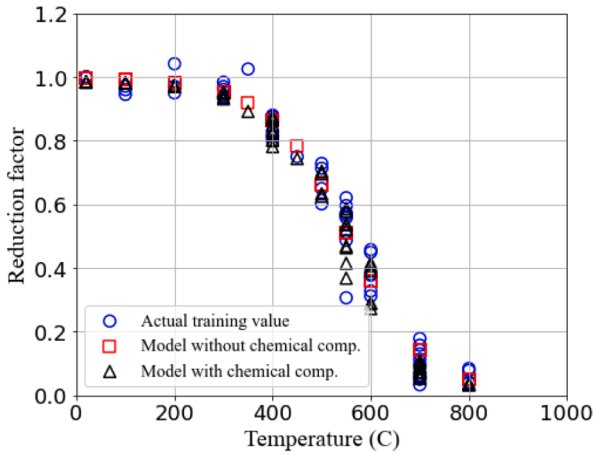

(a) Training data for k_u

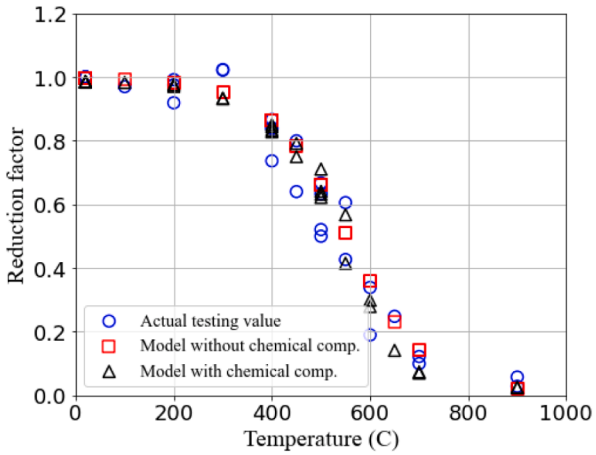

(b) Testing data for k_u

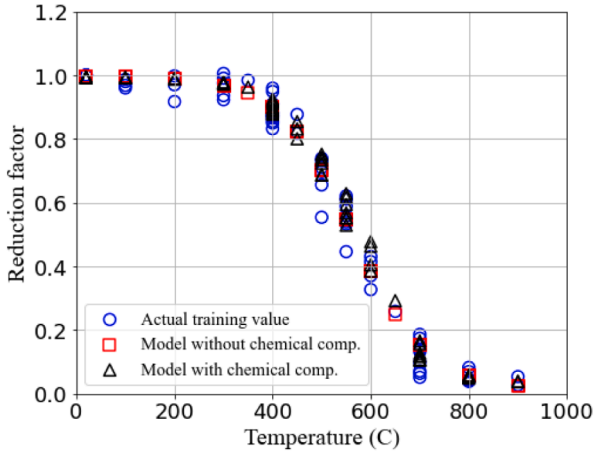

(c) Training data for k_y

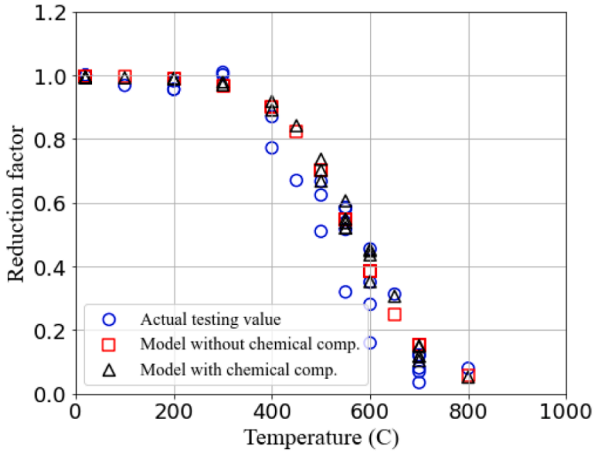

(d) Testing data for k_y

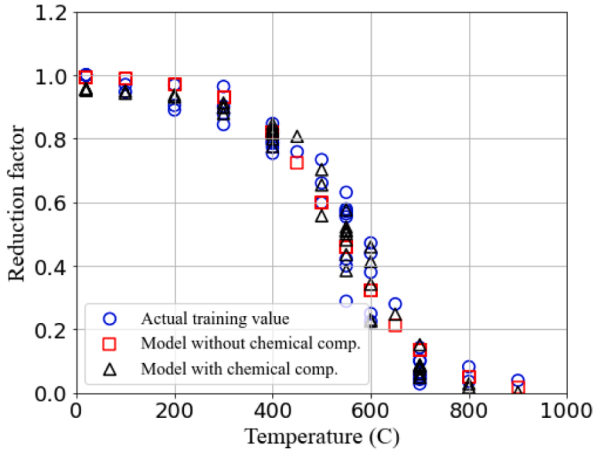

(e) Training data for $k_{0.2}$

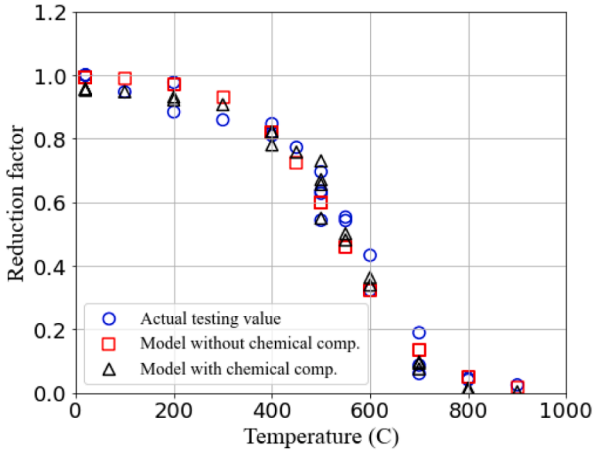

(f) Testing data for $k_{0.2}$

Fig. 13. Accuracy of the developed model for the material reduction factors with temperatures.

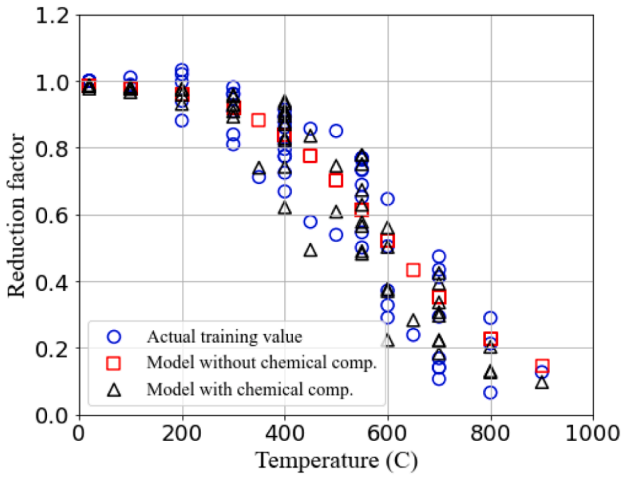

(g) Training data for k_E

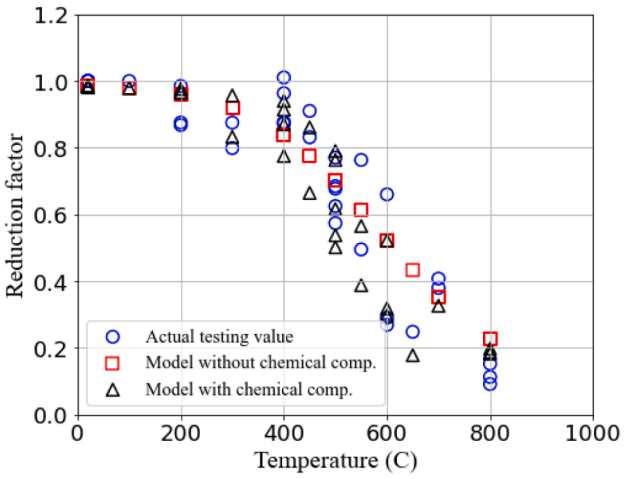

(h) Testing data for k_E

Fig. 13. (*continued*).

Table 3
Comparison between actual and predicted strength reduction factor using simple and multivariate methods for the testing data set.

Temp (°C)	$k_{u,act}$	$k_{u,m}$	$k_{u,s}$	$\rho_{u,m}$%	$\rho_{u,s}$%
400	0.84	0.83	0.87	−1	3
400	0.87	0.85		−2	0
400	0.74	0.83		12	18
400	0.84	0.84		1	3
450	0.80	0.79	0.78	−1	−2
450	0.64	0.75		17	22
500	0.63	0.62	0.66	−2	4
500	0.50	0.64		28	32
500	0.52	0.63		21	27
500	0.67	0.71		6	−1
550	0.43	0.41	0.51	−3	20
550	0.61	0.57		−6	−16
600	0.19	0.30	0.36	57	89
600	0.34	0.28		−18	6
700	0.12	0.07	0.14	−43	16
700	0.10	0.07		−26	42
900	0.06	0.02	0.02	−58	−66
900	0.03	0.03		−12	–32

correlation. This suggests that Ni has a greater impact on the material's ultimate strength at elevated temperatures than other chemical compositions. A similar trend was observed for the prediction of the yield strength reduction factor, but the accuracy of prediction was found to be less affected by the type of chemical composition used in the algorithm. All components were able to predict the reduction factor with similar accuracy, as shown in Fig. 14**(b)**.

9. Discussion

The collected data from the literature elevated temperature test programmes of high strength steels shows significant scatter in the strength and stiffness reduction factors. Thus, predicting the reduction factors merely based on the temperature value and irrespective of the chemical composition underestimates these values leading to potentially overdesigned structural members. The method proposed in the present study informs the design process to make construction practices economical and more sustainable by optimising the steel design at elevated temperatures. Fire testing includes many parameters which may eventually have a profound effect on the results including chemical composition, the heating rate, holding time, and the strain rate of the test. Each of these test parameters can affect the fire performance of high strength steels. There is a lack of uniformity and absence of many test parameters in published works e.g. holding time and strain rate. While the presented methodology which accounts for the chemical compositions is believed to predict the elevated temperatures with a higher accuracy compared with the available methods in the literature, other parameters are of importance as well, and should be considered in future studies. It should be noted that a similar approach to the one presented in this study could be applied to arrive at the optimal chemical compositions that can perform well during the fire by using larger volume of input data and utilizing other ML optimization techniques.

10. Conclusion

The collected data from experimental tests in literature showed that there is a large degree of scatter in the elevated temperature reduction factors of high strength steels (HSS). The manufacturing process of HSS together with their chemical compositions lead to material characteristics and fire performance that are different from those of conventional mild steels. The microstructure of HSS at ambient temperature is the martensite which is not stable and tends to transform to stable ferrite and cementite phases at elevated temperature. The strength of HSS is controlled by the amount of developed cementite which is primarily a function of the chemical composition of the steel and the attained temperature. The present study adopted a machine learning (ML) algorithm of ANN to predict strength and stiffness reduction factors for HSS at elevated temperatures. The developed ML model is trained and validated using collected test data from published literature experimental programmes. Both a multivariate and simple regression analysis were adopted and compared in this paper. The following conclusions were drawn based on the present study:

- Multivariate regression can predict several reduction factors at a specific temperature depending on the chemical compositions while simple regression reports a single prediction at each temperature and results in a significantly large error. For example, the simple regression method predicts ultimate tensile strength reduction factors 67% and 325% higher than the actual value at 500 °C and 700 °C, respectively. Adopting the multivariate method reduces the gap between the predicted and the actual values by predicting

Table 4
Comparison between actual and predicted strength reduction factor using simple and multivariate methods for the training data set.

Temp (°C)	$k_{u,act}$	$k_{u,m}$	$k_{u,s}$	$\rho_{u,m}$%	$\rho_{u,s}$%	Temp (°C)	$k_{u,act}$	$k_{u,m}$	$k_{u,s}$	$\rho_{u,m}$%	$\rho_{u,s}$%
400	0.88	0.82	0.87	−6	−1	**550**	0.57	0.54	0.51	−6	−11
400	0.86	0.87		1	1	**550**	0.31	0.37		20	67
400	0.86	0.80		−7	0	**600**	0.33	0.29	0.36	−12	10
400	0.87	0.87		0	0	**600**	0.31	0.29		−8	15
400	0.83	0.87		6	5	**600**	0.38	0.42		10	−5
400	0.87	0.85		−3	−1	**600**	0.46	0.41		−11	−22
400	0.88	0.83		−6	−2	**600**	0.38	0.27		−29	−6
400	0.80	0.78		−2	8	**600**	0.45	0.39		−13	−20
400	0.81	0.82		1	6	**700**	0.16	0.07	0.14	−54	−10
400	0.82	0.80		−2	6	**700**	0.06	0.09		45	127
450	0.75	0.74	0.78	−1	4	**700**	0.03	0.06		79	325
500	0.73	0.70	0.66	−3	−9	**700**	0.13	0.11		−17	9
500	0.65	0.63		−4	2	**700**	0.18	0.07		−60	−21
500	0.71	0.70		−2	−7	**700**	0.05	0.09		80	181
500	0.60	0.63		5	10	**700**	0.11	0.10		−12	25
550	0.62	0.58	0.51	−7	−18	**700**	0.06	0.05		−5	151
550	0.51	0.46		−10	0	**700**	0.10	0.08		−13	45
550	0.51	0.47		−8	1	**700**	0.14	0.11		−25	0
550	0.57	0.54		−5	−10	**800**	0.04	0.04	0.05	−10	19
550	0.60	0.52		−13	−14	**800**	0.08	0.03		−57	−35
550	0.56	0.59		5	−8	**800**	0.08	0.03		−61	−40
550	0.49	0.41		−15	5	**800**	0.04	0.03		−15	31

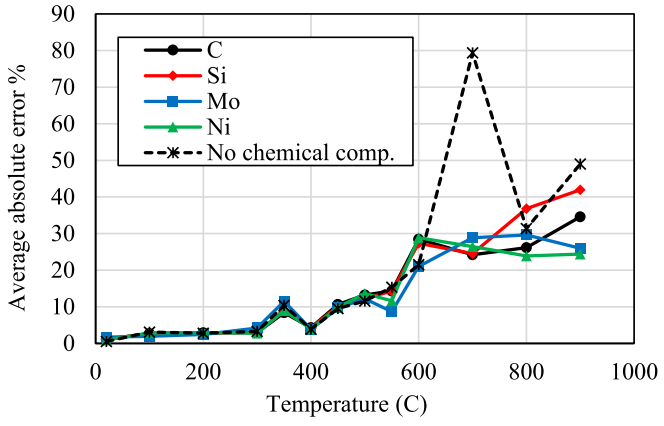

(a) Average absolute error for k_u

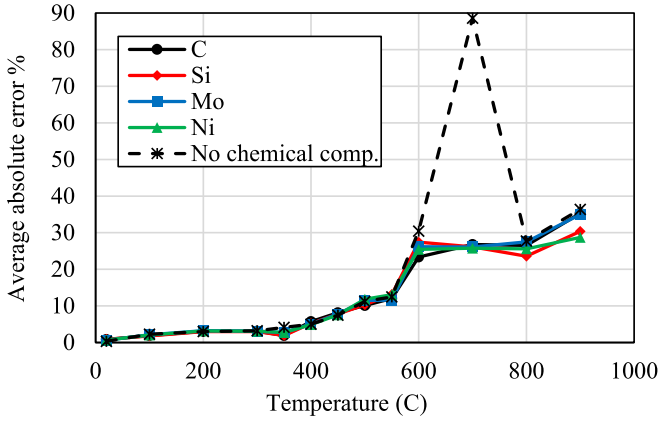

(b) Average absolute error for k_y

Fig. 14. Average absolute error for predating ultimate strength reduction factors when various chemical composition was used in the ML algorithm.

several reduction factors at the same temperature; reducing the absolute errors at 500 °C and 700 °C to 20% and 80%, respectively.

- The strength reduction factors are heavily influenced by the chemical composition at high temperatures, specifically within the temperature range of 600 °C to 900 °C.
- Different chemical compositions predict the ultimate strength reduction factor with varying levels of accuracy at high temperature. The best correlation was found when Ni was individually used in the ML algorithm indicating that Ni has a greater impact on the material's ultimate strength at elevated temperatures than other chemical compositions.
- The method proposed in the present study informs the design process to make construction practices economical and more sustainable by optimising the steel design at elevated temperatures.

Declaration of Competing Interest

The authors declare that they have no known competing financial interests or personal relationships that could have appeared to influence the work reported in this paper.

References

[1] BSI. BS EN 1993-1-1: Eurocode 3: Design of steel structures–part 1–1: general rules and rules for buildings. London, UK: BSI; 2005.
[2] BSI. BS EN 1993-1-12: Eurocode 3: Design of steel structures–part 1–12–additional rules for the extension of EN 1993 up tosteel grades S 700. London, UK: BSI; 2007.
[3] BSI. BS EN 1993-1-2: Eurocode 3: Design of steel structures–part 1–2: general rules–structural fire design. London, UK: BSI; 2005.
[4] The Steel Construction Institute (2020), High strength steel design and execution guide. Publication number: SCI P432. Ascot, UK.
[5] Callister WD, Rethwisch DG. Materials science and engineering. New York: John willey & Sons. Inc; 2007. p. 362–3.
[6] Shaheen MA, Foster AS, Cunningham LS, Afshan S. Behaviour of stainless and high strength steel bolt assemblies at elevated temperatures—A review. Fire Saf J 2020; 113:102975.
[7] Naser MZ. Deriving temperature-dependent material models for structural steel through artificial intelligence. Constr Build Mater 2018;191:56–68.
[8] Desu RK, Krishnamurthy HN, Balu A, Gupta AK, Singh SK. Mechanical properties of Austenitic Stainless Steel 304L and 316L at elevated temperatures. J Mater Res Technol 2016;5(1):13–20.
[9] Qiang X, Bijlaard F, Kolstein H. Dependence of mechanical properties of high strength steel S690 on elevated temperatures. Constr Build Mater 2012;30:73–9.
[10] Qiang X, Bijlaard FS, Kolstein H. Deterioration of mechanical properties of high strength structural steel S460N under steady state fire condition. Mater Des (1980-2015) 2012;36:438–42.

[11] Qiang X. Behaviour of high strength steel endplate connections in fire and after fire. (PhD thesis). 2013.
[12] Chen J, Young B, Uy B. Behavior of high strength structural steel at elevated temperatures. J Struct Eng 2006;132(12):1948–54.
[13] Chiew SP, Zhao MS, Lee CK. Mechanical properties of heat-treated high strength steel under fire/post-fire conditions. J Constr Steel Res 2014;98:12–9.
[14] Choi IR, Chung KS, Kim DH. Thermal and mechanical properties of high-strength structural steel HSA800 at elevated temperatures. Mater Des 2014;63:544–51.
[15] Winful AD, Cashell KA, Afshan S, Barnes AM, Pargeter RJ. Elevated temperature material behaviour of high-strength steel. Proc Inst Civ Eng-Struct Build 2017;170 (11):777–87.
[16] Xiong MX, Liew JR. Mechanical properties of heat-treated high tensile structural steel at elevated temperatures. Thin-Walled Struct 2016;98:169–76.
[17] Li GQ, Jiang SC, Yin YZ, Chen K, Li MF. Experimental studies on the properties of constructional steel at elevated temperatures. J Struct Eng 2003;129(12):1717–21.
[18] Wang W, Wang K, Kodur V, Wang B. Mechanical properties of high-strength Q690 steel at elevated temperature. J Mater Civ Eng 2018;30(5):04018062.
[19] Huang L, Li GQ, Wang XX, Zhang C, Choe L, Engelhardt M. High temperature mechanical properties of high strength structural steels Q550, Q690 and Q890. Fire Technol 2018;54(6):1609–28.
[20] Jiang J, Bao W, Peng ZY, Wang YB, Liu J, Dai XH. Experimental investigation on mechanical behaviours of TMCP high strength steel. Constr Build Mater 2019;200: 664–80.
[21] Li GQ, Song LX. Mechanical properties of TMCP Q690 high strength structural steel at elevated temperatures. Fire Saf J 2020;116:103190.
[22] Neuenschwander M, Scandella C, Knobloch M, Fontana M. Modeling elevated-temperature mechanical behavior of high and ultra-high strength steels in structural fire design. Mater Des 2017;136:81–102.
[23] Shakil S, Lu W, Puttonen J. Experimental studies on mechanical properties of S700 MC steel at elevated temperatures. Fire Saf J 2020;116:103157.
[24] Wang W, Zhang Y, Xu L, Li X. Mechanical properties of high-strength Q960 steel at elevated temperature. Fire Saf J 2020;114:103010.
[25] Xiong MX, Liew JR. Experimental study to differentiate mechanical behaviours of TMCP and QT high strength steel at elevated temperatures. Constr Build Mater 2020;242:118105.
[26] Schneider R, Lange J. Constitutive equations and empirical creep law of structural steel S460 at high temperatures. J Struct Fire Eng 2011.
[27] Lange J, Wohlfeil N. Examination of the mechanical properties of steel S460 for fire. J Struct Fire Eng 2010.
[28] Moolayil J, Moolayil J, John S. Learn Keras for deep neural networks. Birmingham: Apress; 2019. p. 1–192.